Supplementary Information for

Catalytic 'Gelectrodes' Based on Co and Ni-Fe Oxy/Hydroxides for Sustainable and Enhanced Oxygen Evolution Reaction

Anu Bovas, T. P. Radhakrishnan*

School of Chemistry, University of Hyderabad, Hyderabad – 500 046, India

*Email: tpr@uohyd.ac.in

Experimental details

***Materials*:** The materials used in the fabrication of the electrocatalyst and the gelectrode, and the electrochemical experiments include, cobalt (II) nitrate hexahydrate (Sigma-Aldrich, 98%), urea (Rankem, 99.5%), sodium hydroxide (Finar, 97%), iron (III) chloride (Sigma-Aldrich, >97%), chitosan (CS, Sigma-Aldrich, MW_{av} = 50-190 kDa), poly(acrylamide-*co*-acrylic acid) (PAM, Aldrich, MW_{av} = 5 kDa, water 10-15%), polyacrylic acid (PAA, Fluka, MW_{av} = 170 kDa, sodium salt), poly(2-hydroxyethyl methacrylate) (PHEMA, Sigma-Aldrich, MW_{av} = 20 kDa), Nafion (Sigma-Aldrich, 5 wt% perfluorinated resin solution in lower aliphatic alcohols and water), poly-*L*-lysine solution (PLL, Sigma-Aldrich, 0.1% w/v in water), potassium hydroxide (Merck, Emparta Grade), Milli-Q water (ambient temperature resistivity = 18 MΩ cm), and nickel foam (NF, BAT-SOL Equipments and Technology, thickness ~ 1 mm, density ≥ 250 g m^{-2}, porosity = 110 ppi).

***Synthesis of* $Ni_{1-x}Fe_x(OH)_y$*/NF*:**[S1] NF was cut into 2×0.5 cm^2 pieces and sonicated in 1 M HCl for 10 min to remove the surface oxide layer, and then ultrasonicated in Milli-Q water and absolute ethanol sequentially. The cleaned NF was dipped in 50 mM $FeCl_3$ aqueous solution for 10 s; it was then heated in an oven at 300 °C for 30 min.

***Synthesis of CoOOH*:**[S2] 0.145 g (0.5 mmol) cobalt (II) nitrate hexahydrate and 1.50 g (25 mmol) urea were dissolved in 60 mL water. 10 mL of a freshly prepared solution of 1 M NaOH was added; color of the solution mixture changed from blue to brown. It was stirred at 25 °C for 30 min; the precipitated CoOOH was washed several times with water and ethanol, and dried in an oven at 60 °C for 10 h.

***Fabrication of gelectrodes*:** **$Ni_{1-x}Fe_x(OH)_y$-CS/NF** was fabricated by drop-casting a 25 mg mL^{-1} solution of chitosan (CS) in 1% acetic acid on $Ni_{1-x}Fe_x(OH)_y$/NF. **CoOOH-CS/NF** was fabricated as follows. 4 mg of CoOOH was dispersed in 1 mL of the CS solution (weight ratio, Co/CS ~ 0.1) and stirred for 1 h. A 2×0.5 cm^2 piece of NF was dipped into this solution, kept for 10 min and then dried at 25 °C; the coated area was 0.6×0.5 cm^2. This procedure was repeated thrice to obtain CoOOH-CS/NF. Similar procedure was adopted using other polymers PAM, PAA, PHEMA, Nafion and poly-L-lysine to get the corresponding $Ni_{1-x}Fe_x(OH)_y$-polymer/NF and CoOOH-polymer/NF gelectrodes used in the control experiments.

***Characterization*:** Elemental composition was determined by inductively coupled plasma – optical emission spectroscopy (ICP-OES) using a Varian Model 720-ES ICP-OES. Samples for the analysis were prepared by dissolving the catalytic electrode in a 1:3 v/v mixture of conc. HNO_3 and conc. H_2SO_4. X-ray photoelectron spectroscopy (XPS) was carried out using a Thermo Scientific Model MULTILAB 2000 Base system with a twin anode Al source equipped

with a hemispherical analyzer; the binding energies are referenced to the C1s peak at 284.8 eV. Carl Zeiss model Merlin Compact FE-SEM equipped with an Oxford Instruments X-Max^N SDD (50 mm^2) was used for field emission scanning electron microscope (FE-SEM) imaging and energy dispersive X-ray (EDX) spectroscopy; the data was analyzed using the INCA software (ver. 4.13). Transmission electron microscopy (TEM) imaging and selected area electron diffraction (SAED) were carried out using a JEOL model JEM-F200/F2 multipurpose TEM; the samples were prepared by sonicating the catalytic electrode in water to separate the nanocomposite thin film from the NF and dip-coating the solution on carbon-coated copper grids. Powder X-ray diffraction patterns were recorded on a Bruker D8 Advance X-ray diffractometer using Cuk$_\alpha$ radiation of λ = 1.54184 Å at 30 mA and 40 kV.

***Electrochemical Experiments*:** Metrohm Autolab model PGSTAT204 FRA32M and Ametek Scientific Instruments model PARSTAT MC 1000 electrochemical workstations were used to carry out the electrochemical experiments; the precision of both current and potential measurements was ±0.2%. A 3-electrode system with the nanocomposite thin film coated on NF (gelectrode) as the working electrode, Hg/HgO as the reference electrode and Pt coil as the counter electrode were set up to perform cyclic voltammetry (CV) and linear sweep voltammetry (LSV). All experiments were carried out at 25 °C with 1 M KOH (measured pH = 13.8) as the electrolyte, typically at a scan rate of 10 mV s^{-1}. The electrode potentials were converted with respect to reversible hydrogen electrode (RHE), using the formula E (*vs* RHE) = E (*vs* Hg/HgO) + 0.105 + 0.0591×pH; precision of the overpotentials reported is ~ ±5 mV. The values obtained are reported without iR correction. Tafel plots (overpotential *vs* log| j|, where j = current density) were prepared from the cathodic half cycles of the CV to avoid the oxidation peak of Ni^{2+} to Ni^{3+}, with least square fit to a straight line in the Faradaic region; precision of the Tafel slopes reported is ±3 mV dec^{-1}. CV was carried out at different scan rates, and the slope of the plot of $\Delta j/2$ (Δj = anodic current density – cathodic current density) *vs* scan rate provided the double layer capacitance from which the electrochemically active surface area (ECSA) was calculated. Faradaic efficiency was determined by the volume displacement method using a 2-electrode system (working and counter electrodes), collecting the O_2 gas by displacement of the KOH electrolyte in a graduated column (precision of the volume measurements was ±0.05 mL), and estimating the ratio of the number of mols of the gas produced experimentally to the theoretically calculated value. Chronopotentiometry and chronoamperometry were carried out for 100 h and 50 h, respectively, to explore the stability of gelectrodes. It was noted that during the extended stability test, 1-2 mL of water was electrolyzed, and was replenished. Turn-over-frequency (TOF) of the system for OER was calculated from the equation TOF = $jA/4Fm$, where j = current density, A = geometric area of the catalytic electrode, F = Faraday constant, and m = number of mols of the catalyst. The cell voltage of a 2-electrode system with Pt as the counter electrode was explored using polarization plots to study the overall electrochemical water splitting; durability of the system was monitored for 24 h using chronoamperometry plot at an applied voltage of 4 V.

Scanning electron microscopy and EDX spectroscopy

Figure S1. FE-SEM images of **(a, b)** CoOOH-CS/NF and **(c, d)** $Ni_{1-x}Fe_x(OH)_y$-CS/NF at different magnifications.

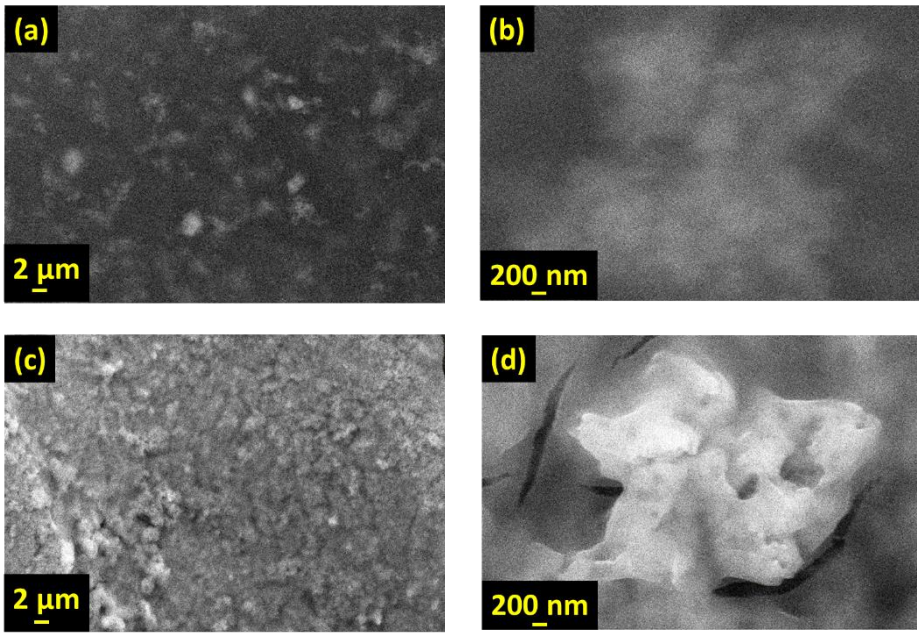

Figure S2. FE-SEM (inset: EDX histogram) images of **(a, b)** CoOOH-CS/NF and **(c, d)** $Ni_{1-x}Fe_x(OH)_y$-CS/NF at different magnifications.

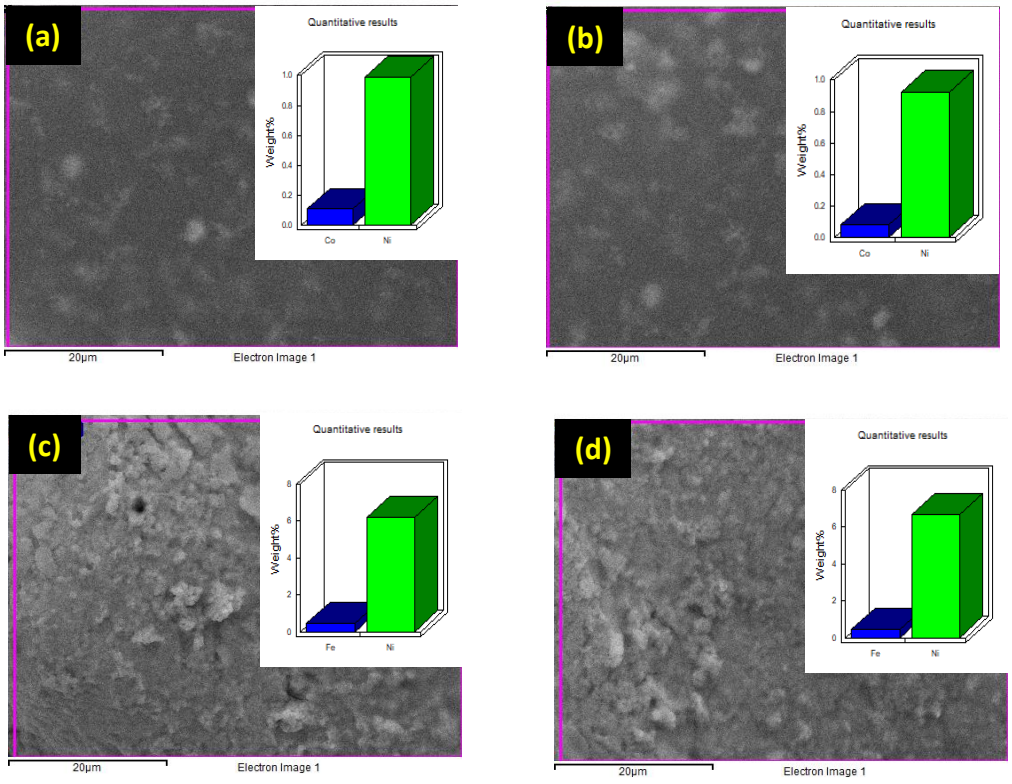

Table S1. Atomic% of relevant elements (from EDX spectra) in the CoOOH-CS/NF and $Ni_{1-x}Fe_x(OH)_y$-CS/NF nanocomposite thin films.

CoOOH-CS/NF	**Atomic%**		**$Ni_{1-x}Fe_x(OH)_y$-CS/NF**	**Atomic%**	
Co	9.52	7.60	**Fe**	7.36	6.52
Ni	90.48	92.40	**Ni**	92.64	93.48

Transmission electron microscopy and SAED

Figure S3. (a) TEM image (scale bar = 100 nm), **(b)** HR-TEM image showing the lattice plane spacing (scale bar = 10 nm), and **(c)** electron diffraction pattern of as-prepared CoOOH-CS. **(d-f)** The corresponding images after 100 h of chronopotentiometry at 50 mA cm^{-2}, and **(g-i)** after 50 h of chronoamperometry at 3 V *vs* RHE.

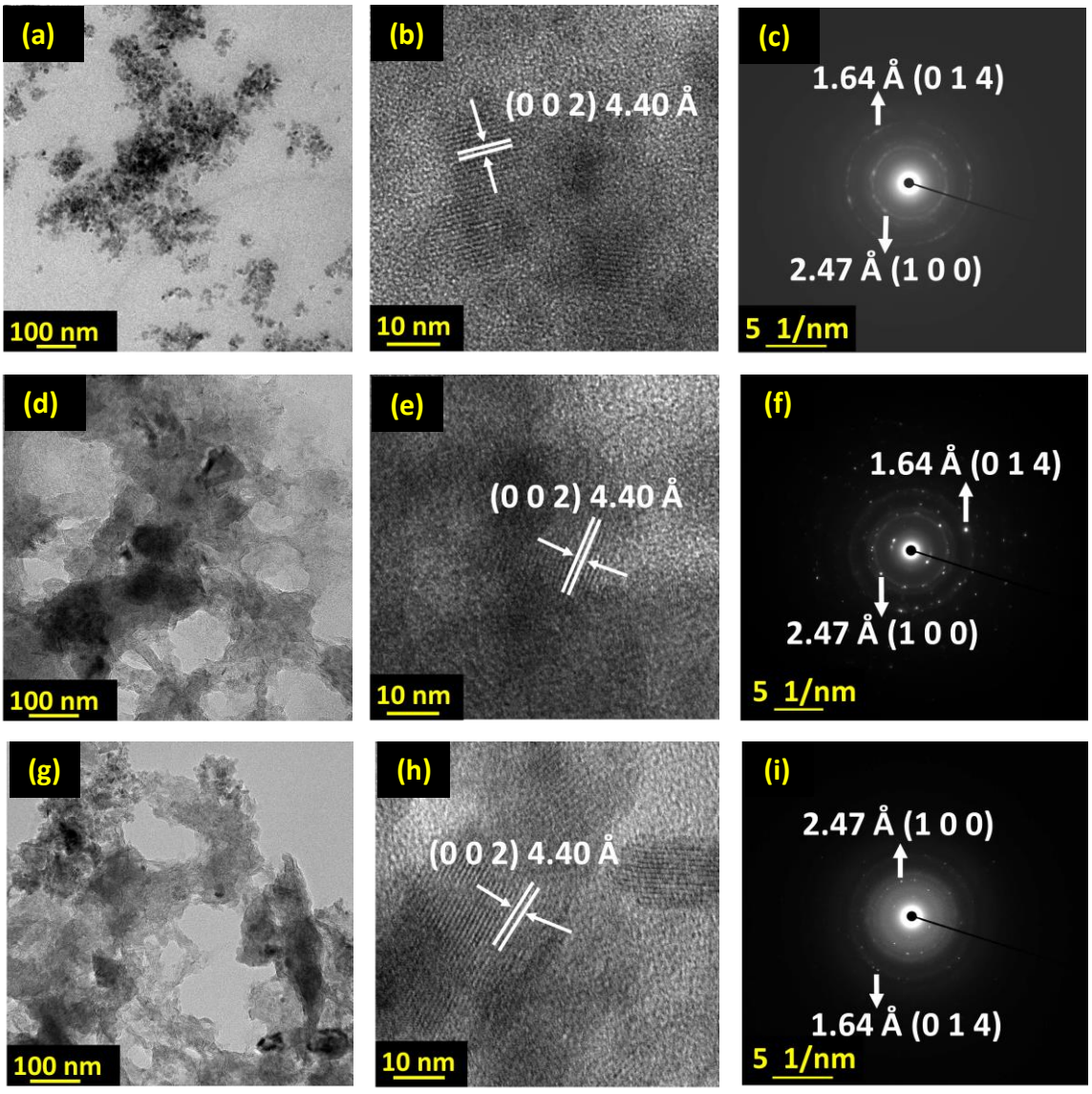

Figure S4. (a) TEM image (scale bar = 100 nm), **(b)** HR-TEM image showing the lattice plane spacing (scale bar = 10 nm), and **(c)** electron diffraction pattern of as-prepared $Ni_{1-x}Fe_x(OH)_y$-CS. **(d-f)** The corresponding images after 100 h of chronopotentiometry at 50 mA cm^{-2}, and **(g-i)** after 50 h of chronoamperometry at 3 V *vs* RHE.

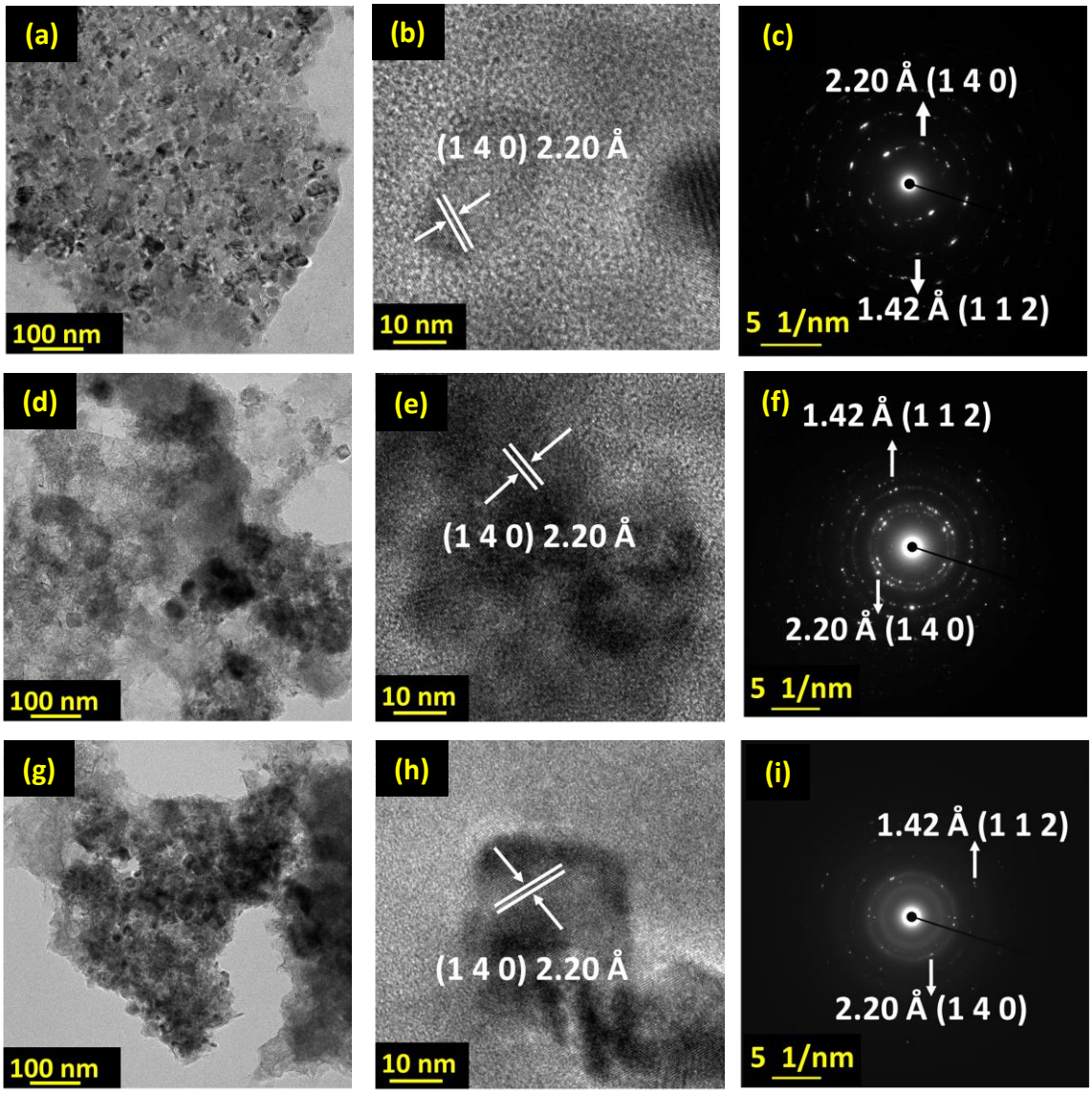

Powder x-ray diffraction

Figure S5. Powder X-ray diffraction pattern of CoOOH and CoOOH-CS compared to the reported pattern (crystallography open database number: 96-900-9885).

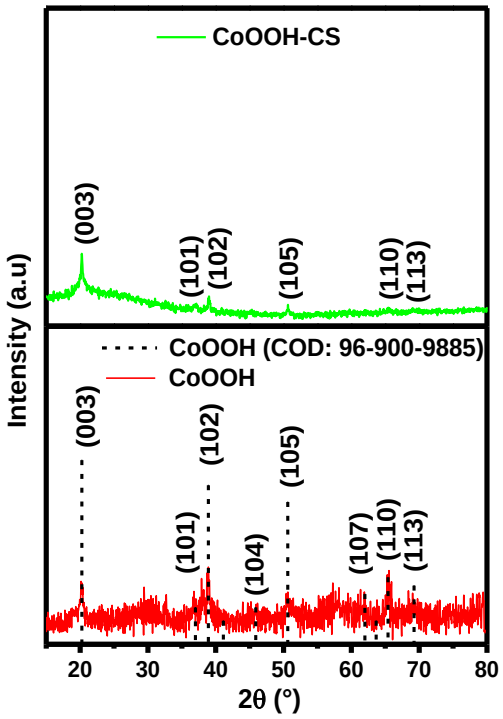

X-ray photoelectron spectroscopy

Figure S6. Survey spectra of **(a)** CoOOH **(b)** $Ni_{1-x}Fe_x(OH)_y$-CS/NF. Core level O 1s XPS of **(c)** CoOOH **(d)** $Ni_{1-x}Fe_x(OH)_y$-CS/NF indicating the relevant spectral deconvolutions. The experimental spectra (black line), the total fitting (red line) and individual components are indicated.[S3]

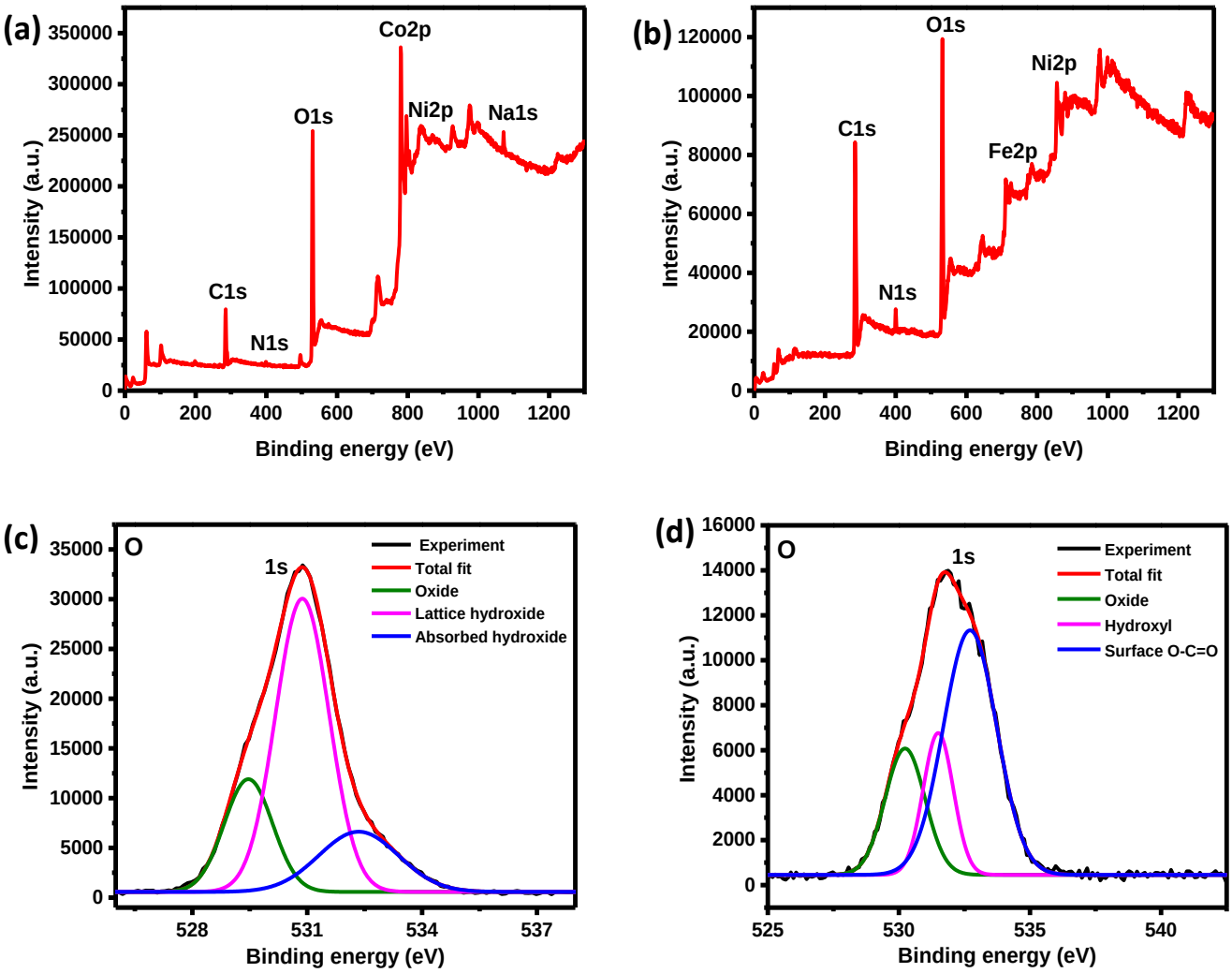

Table S2. Comparison of the relevant XPS peaks of **(a)** Co and **(b)** O of CoOOH with those reported earlier.[S3]

(a)

Co		**Reported (eV)**	**Observed (eV)**
$2p_{3/2}$	Co^{2+}	781.0	781.4
	Co^{3+}	779.8	780.1
	Satellite peak		785.7
$2p_{1/2}$	Co^{2+}	796.5	796.7
	Co^{3+}	795.0	794.9
	Satellite peak		802.9

(b)

O 1s	**Reported (eV)**	**Observed (eV)**
Lattice O	529.8	529.5
Lattice OH	530.7	530.9
Absorbed OH	531.7	532.3

Table S3. Comparison of the relevant XPS peaks of **(a)** Ni, **(b)** Fe and **(c)** O respectively of $Ni_{1-x}Fe_x(OH)_y$-CS/NF with those reported earlier.[S3-S5]

(a)

Ni		**Reported (eV)**[S4]	**Observed (eV)**
$2p_{3/2}$	Ni^{2+}	855.8	855.9
	Ni^{3+}	853.2	
	Satellite peak	861.0	861.5
$2p_{1/2}$	Ni^{2+}	873.6	873.4
	Ni^{3+}	870.4	
	Satellite peak	879.4	879.4

(b)

Fe		**Reported (eV)**[S5]	**Observed (eV)**
$2p_{3/2}$	Fe^{2+}	711.4	711.0
	Fe^{3+}	714.8	713.2
$2p_{1/2}$	Fe^{2+}	724.3	724.5
	Fe^{3+}	727.7	726.5

(c)

O 1s	**Reported (eV)**[S3]	**Observed (eV)**
Lattice O	529.8	529.5
Absorbed OH (A_{OH})	531.7	531.5
Surface O-C=O ($S_{O-C=O}$)	532.7	532.7

Electrochemical setup

Figure S7. (a) The electrochemical measurement setup of the 3-electrode system with the nanocomposite thin film coated on NF (gelectrode) as the working electrode, Hg/HgO as the reference electrode and Pt coil as the counter electrode. **(b)** Photograph of a gelectrode used in the present study.

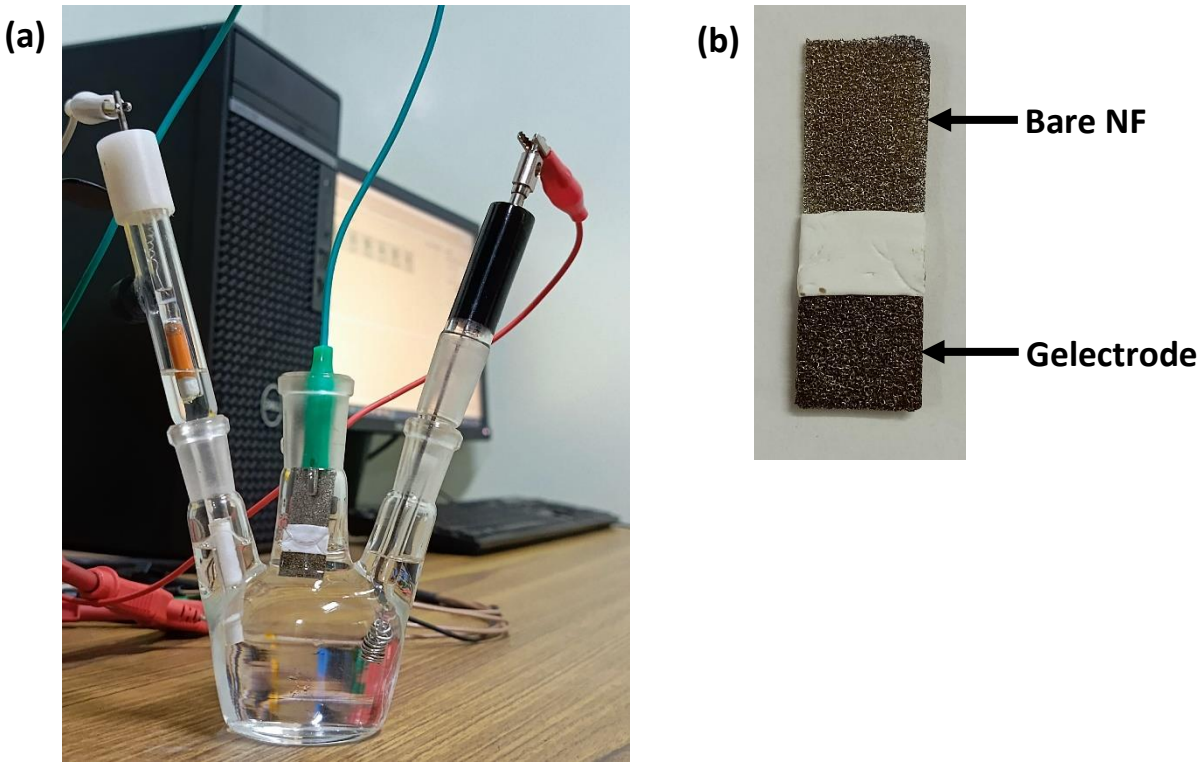

Figure S8. Polarization plots for the OER using **(a)** CoOOH-CS/NF and **(b)** $Ni_{1-x}Fe_x(OH)_y$-CS/NF with reference catalytic electrodes (with different polymers as the binder).

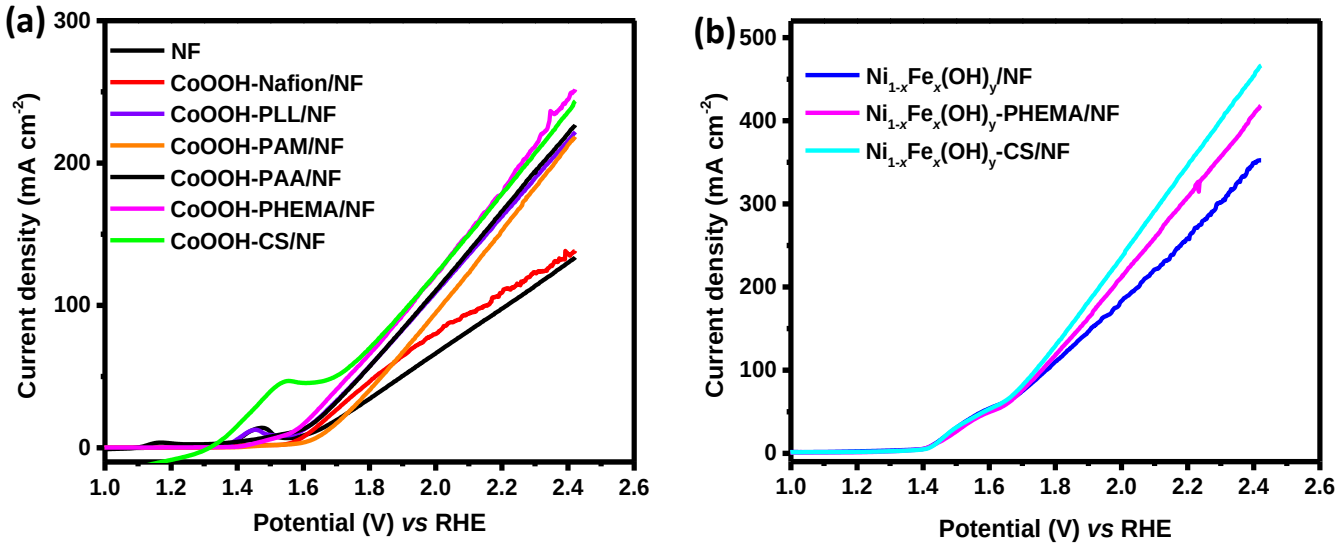

Swelling characteristics of CS under different pH conditions

Figure S9. **(a)** Weight of the chitosan film coated on NF on dipping in aqueous medium with different pH for ~ 20 min, taking out, and subsequently allowing it to dry under ambient atmosphere at 25 °C. **(b)** The corresponding swelling ratio $S = \frac{w_t - w_0}{w_0}$ as a function of time, t; w_0 is the weight of the film in the dry state before dipping, and w_t are the weights immediately after dipping and taking out (t = 0) and at different times when left to dry.

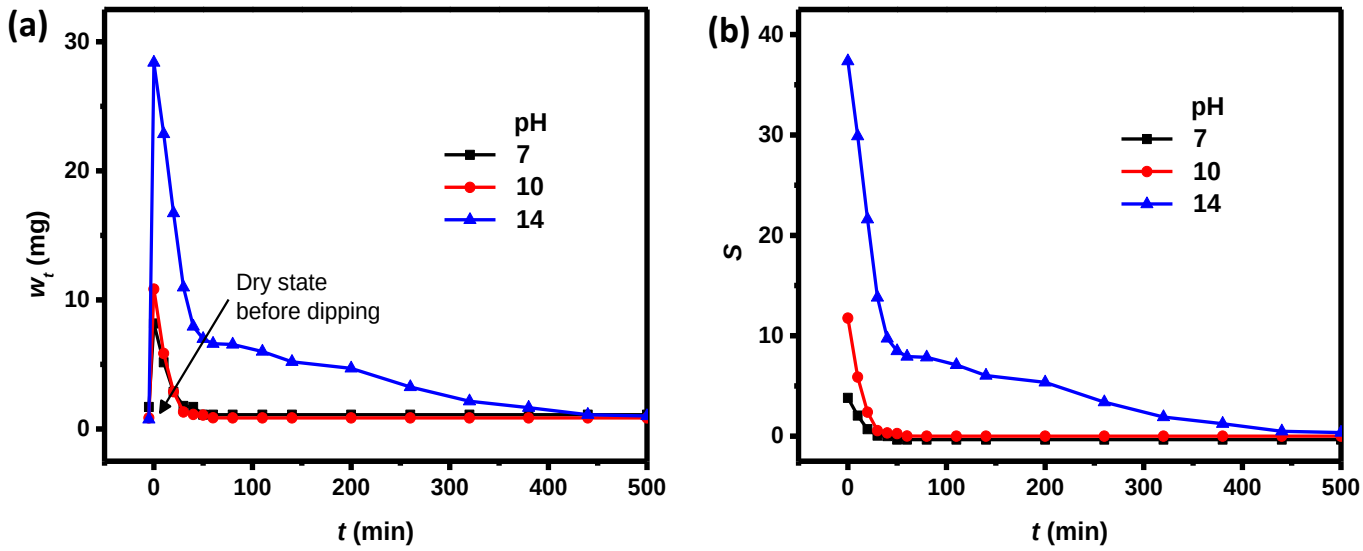

The increase in weight upon dipping indicates the amount of electrolyte absorbed, and the drying stage shows the amount of it retained by the swollen gel over a period of time. Under an acidic pH, not only is the swelling of CS very poor, but it tends to dissolve in the electrolyte making it ineffective as a stabilizing agent. The swelling is better under neutral pH conditions, but it is highest at pH ~ 14 which is the case with the 1 M KOH electrolyte used in the OER reactions in our study.

Characterization of the aerophobic nature of gelectrodes

Figure S10. Photographs of the CoOOH based **(a)** electrode and **(b)** gelectrode during the electrocatalytic O_2 evolution upon applying 2 V *vs* RHE for 10 min. See also the corresponding movie files, Movie1.mp4 and Movie2.mp4.

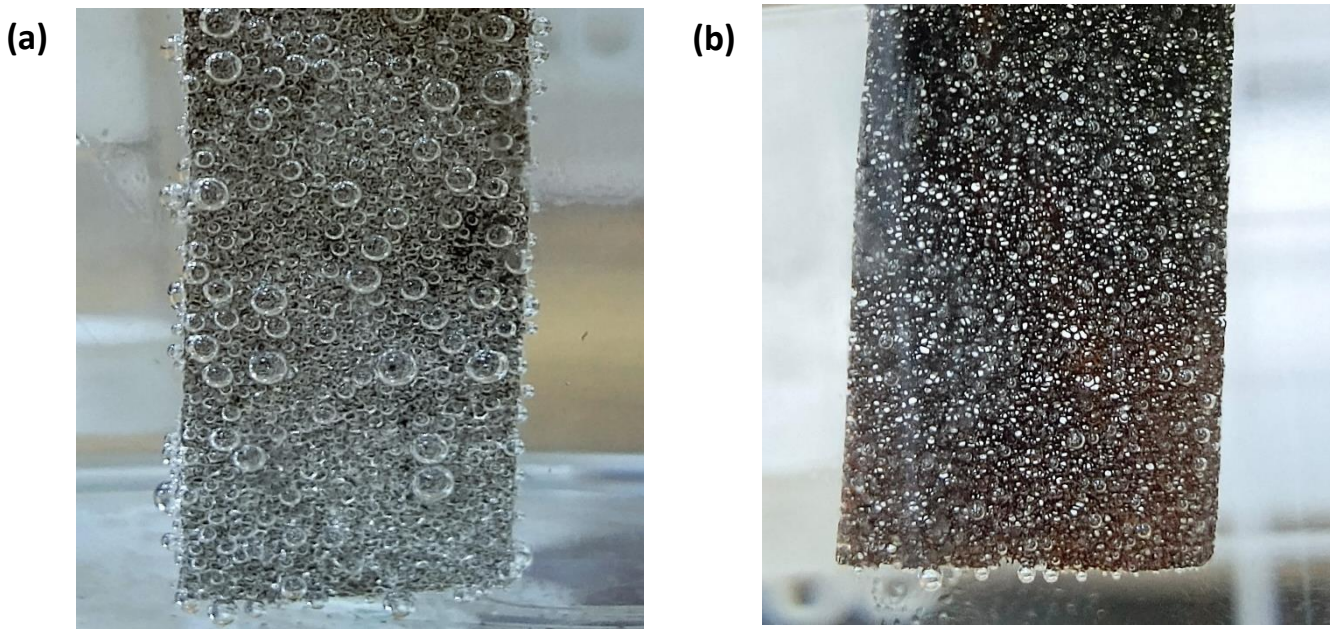

Figure S11. Volume of O_2 *vs* time with the CoOOH based nanocomposite thin film electrode (CoOOH-Nafion/NF) and gelectrode (CoOOH-CS/NF) upon the application of 5 mA current for 30 min (see also Figures 4c, S13); least square fit to a straight line is shown in each case.

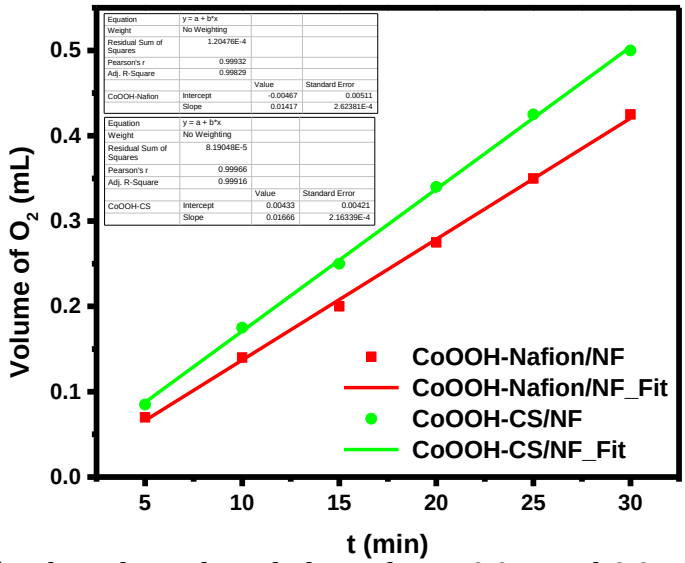

The slope (d*V*/d*t*) for the gelectrode and electrode are 0.017 and 0.014 respectively, indicating the higher gas production rate with the former due to the aerophobic hydrogel coating. Similar trends are seen with the $Ni_{1-x}Fe_x(OH)_y$ based electrode and gelectrode.

Figure S12. CV plots at different scan rates using the different electrodes used to prepare the plots in Figure 4b in the main text: **(a)** Nickel foam **(b)** CoOOH-Nafion/NF **(c)** CoOOH-CS/NF **(d)** $Ni_{1-x}Fe_x(OH)_y$/NF, and **(e)** $Ni_{1-x}Fe_x(OH)_y$-CS/NF.

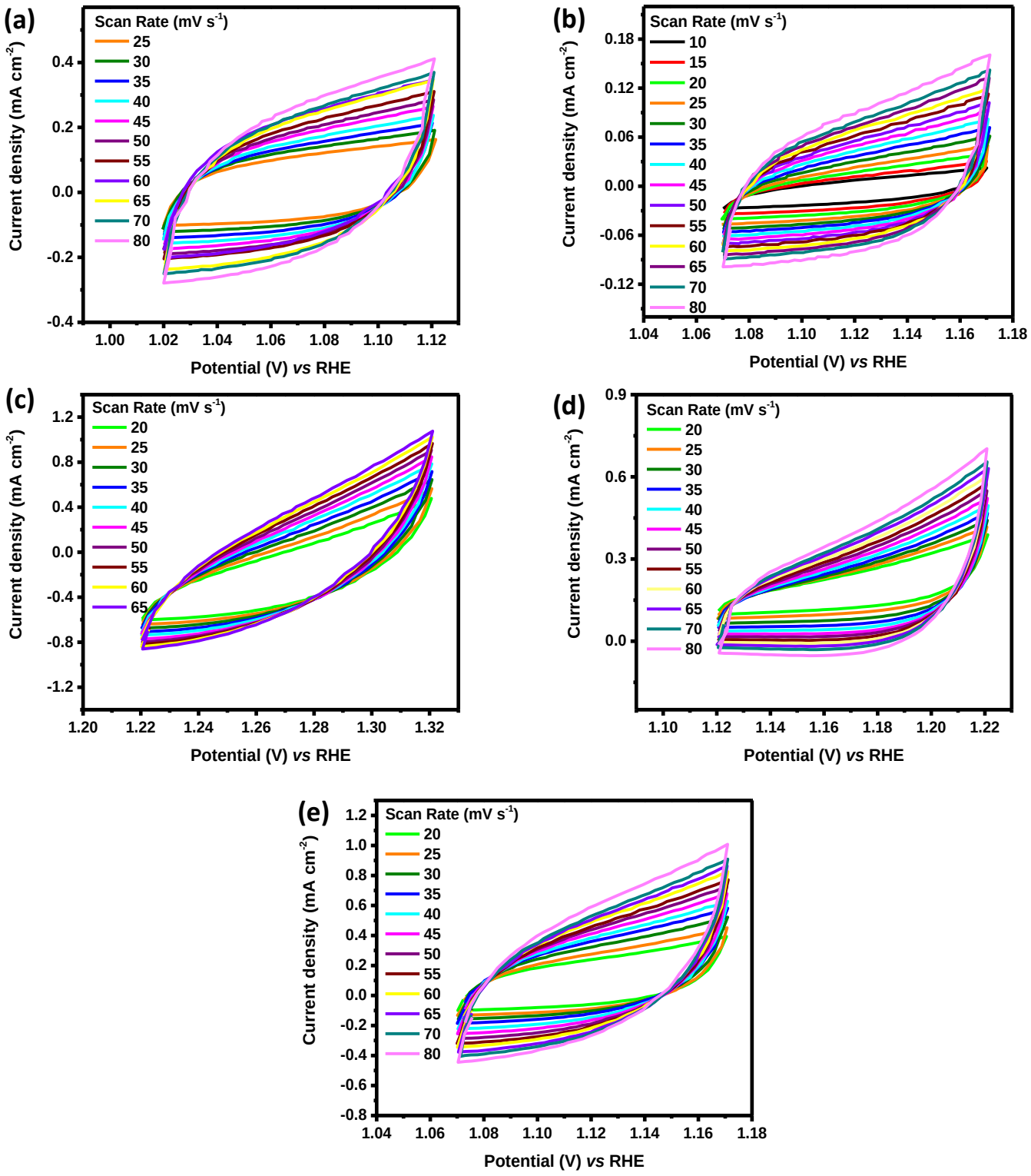

Table S4. Double layer capacitance (C_{dl}) and estimated electrochemically active surface area (ECSA).

Catalyst	C_{dl} (mF cm^{-2})	ECSA (cm^2)
NF	2.49	18.7
CoOOH-Nafion/NF	1.02	7.65
CoOOH-CS/NF	4.46	33.5
$Ni_{1-x}Fe_x(OH)_y$/NF	2.64	19.8
$Ni_{1-x}Fe_x(OH)_y$-CS/NF	4.62	34.7

Calculation of C_{dl} and ECSA

C_{dl} (mF cm^{-2}) = Slope of the plot of $\Delta j/2$ (mA cm^{-2}) *vs* Scan rate (mV s^{-1})

Geometric area (A) of the active electrode = 0.5×0.6 cm^2

C_s of smooth surface (Ni foam)[S6] = 40 μF cm^{-2}

ECSA (cm^2) = C_{dl} (mF cm^{-2}) × A (cm^2) / [C_s (μF cm^{-2}) ×10^{-3}]

Figure S13. Quantity of oxygen produced by 5 mA current as a function of time, using different electrodes; the corresponding Faradaic efficiencies are shown in Figure 4c in the main text.

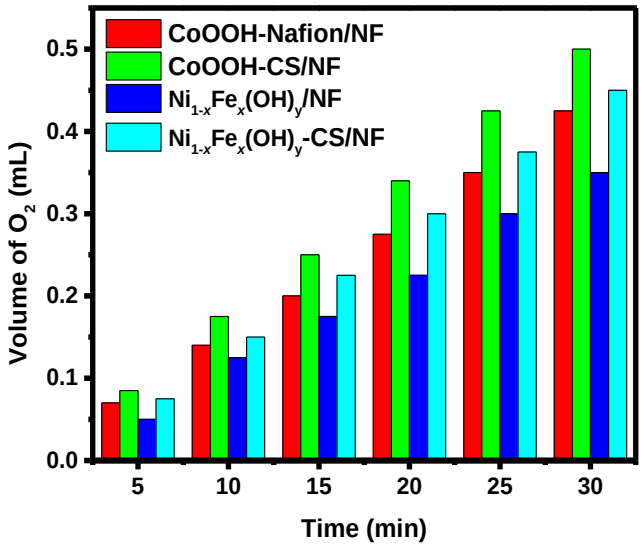

Figure S14. Chronoamperometry plots for the OER carried out at 3 V *vs* RHE using the CoOOH and $Ni_{1-x}Fe_x(OH)_y$ based catalytic electrodes.

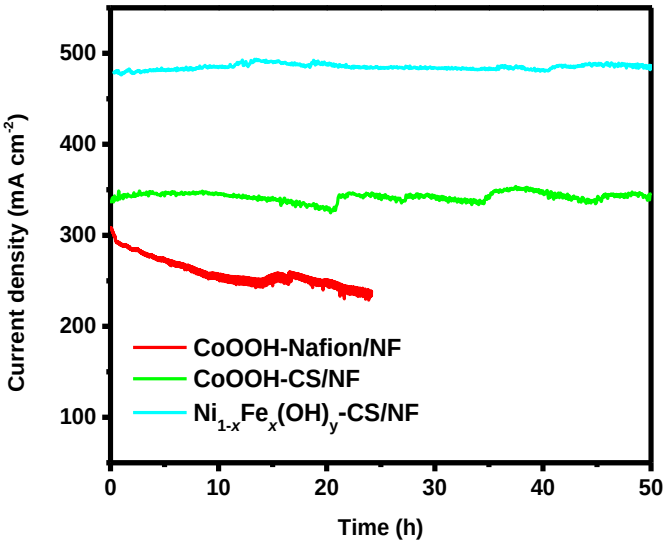

Elemental analysis using ICP

The steps used for the estimation of Co and Fe present in the respective nanocomposite thin films, using the data from ICP-OES analysis are described below; samples for the analysis were prepared by dissolving in conc. HNO_3 + conc. H_2SO_4 and diluting to 100 mL.

CoOOH-CS/NF

Preparation of the nanocomposite film:

Volume of CS solution used = 1 mL (250 mg in 10 mL of 1% acetic acid solution)

∴Weight of CS used = 25 mg

Weight of CoOOH used = 4 mg (Weight ratio, Co/CS used in the film fabrication ~ 0.1)

Weight of the CoOOH + CS film used for the ICP analysis = 2.6 mg

∴Weight of Co (expected) = 0.229 mg

Weight of Co (experimentally found) = **0.203 mg**

$Ni_{1-x}Fe_x(OH)_y$-CS/NF

Molecular mass of $FeCl_3$ = 162.2 g mol^{-1}

Weight of $FeCl_3$ coated on nickel foam = 0.25 mg

∴Weight of Fe present (expected) = 0.086 mg

Weight of Fe (experimentally found) = **0.082 mg**

These data together with the analysis results for the gelectrodes after chronopotentiometry and chronoamperometry are presented in Table S5.

Table S5. Content of Co and Fe in the respective nanocomposite thin films (as prepared, and after chronopotentiometry (CP) and chronoamperometry (CA) runs) determined using ICP-OES analysis. w_{CoOOH} = weight of CoOOH coated (with CS) on the nickel foam (NF) to make the gelectrode; w_{FeCl_3} = weight of $FeCl_3$ coated on the NF to make the gelectrode; w_{Co}= weight of Co; w_{Fe}= weight of Fe (Expected: based on the amount of CoOOH or $FeCl_3$ originally coated on the NF; Found: from ICP analysis of the samples as prepared, and after CP or CA).

w_{CoOOH} **(mg)**	**CoOOH-CS/NF**	w_{Co} (mg)	
		Expected	**Found**
2.60	As prepared	0.229	0.203
1.80	After 100 h of CP @ 50 mA cm^{-2}	0.156	0.153
5.88	After 50 h of CA @ 3 V *vs* RHE	0.511	0.502

w_{FeCl_3} **(mg)**	**$Ni_{1-x}Fe_x(OH)_y$-CS/NF**	w_{Fe} (mg)	
		Expected	**Found**
0.25	As prepared	0.086	0.082
0.30	After 100 h of CP @ 50 mA cm^{-2}	0.103	0.101
0.35	After 50 h of CA @ 3 V *vs* RHE	0.120	0.116

Calculation of TOF for OER

CoOOH-CS/NF

Weight of Co present = 0.203 mg

No. of mols of Co = 3.45×10^{-6}

Current density at 1.449 V *vs* RHE = 20 mA cm^{-2}

Geometric area of the electrode used for this experiment = 0.5×0.6 cm^2

Current flown = 6 mA

TOF = $I/4Fm$ = $(6\times10^{-3}\times3600)/(4\times96485\times3.45\times10^{-6})$ = **16.2 h^{-1}**

$Ni_{1-x}Fe_x(OH)_y$-CS/NF

Weight of Fe present experimentally = 0.082 mg

No. of mols of Fe = 1.47×10^{-6}

Current density at 1.456 V *vs* RHE = 20 mA cm^{-2}

Geometric area of the electrode used for this experiment = 0.4×0.5 cm^2

Current flown = 4 mA

TOF = $I/4Fm$ = $(4\times10^{-3}\times3600)/(4\times96485\times1.47\times10^{-6})$ = **25.4 h^{-1}**

Electrochemical impedance spectroscopy

Impedance spectroscopy was carried out using the FRA32M module of the PGSTAT204 workstation; 10 frequencies (ω) per decade in the range of 0.1 MHz to 0.01 Hz were scanned employing an amplitude of 0.08 V_{RMS}. Data fitting was carried out using the Nova software (ver. 2.1.6).

Figure S15. Nyquist plots for the OER using bare nickel foam (NF) and the Co and Ni-Fe based electrodes and gelectrodes; the equivalent Debye circuit and the nonlinear data fitting are shown. Inset: plots for the electrodes and gelectrodes with smaller axes scale for more clarity. The x:y scale ratios are maintained 1:1 in both the plots.

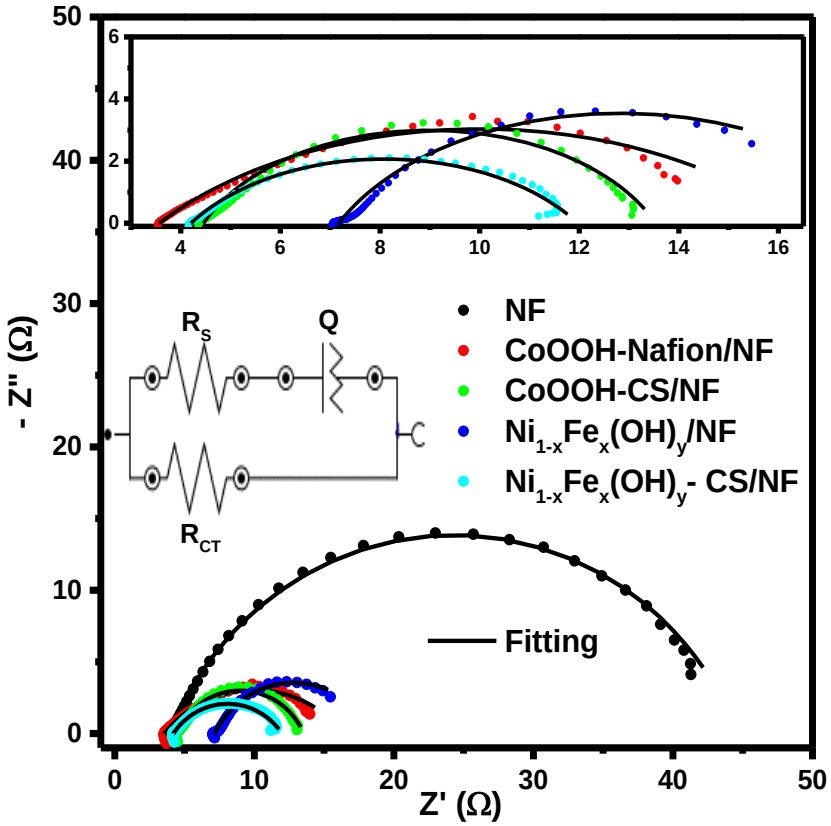

Table S6. The solution (R_S) and charge transfer (R_{CT}) resistances, and the constant phase element (Q) required to fit the Nyquist plots in Figure S15; the correlation coefficient (r) for the fitting are also listed.

Electrode/Gelectrode	R_S (Ω)	R_{CT} (Ω)	Q (mS s^n) [n]	r
NF	4.35	44.6	22.8 [0.761]	0.999
CoOOH-Nafion/NF	4.55	16.4	57.3 [0.561]	0.986
CoOOH-CS/NF	6.64	13.5	22.0 [0.742]	0.991
$Ni_{1-x}Fe_x(OH)_y$/NF	11.70	18.5	121.0 [0.712]	0.996
$Ni_{1-x}Fe_x(OH)_y$-CS/NF	6.48	12.0	14.3 [0.623]	0.990

Comparison of the present catalysts with earlier reported ones

Table S7. Comparison of relevant electrochemical characteristics of the present catalytic electrodes with similar earlier reported ones in KOH electrolyte.

	Maximum current density shown (mA cm^{-2})	**Overpotential (mV) (η_{10})**	**Cell Voltage (V) for 10 mA cm^{-2}**	**Tafel slope (mV dec^{-1})**	**ECSA (cm^2)**	**TOF (s^{-1})**	**Stability (h)**	**Reference**
Co based catalysts								
γ-CoOOH nanosheets	50	300	#	38	#	0.09	13	S7
PNC/Co	300	370	1.64	76	#	#	10	S8
Nanostructured NiCo with oxide layer	320	287	1.52	39	#	#	20	S9
0.7-Co@NG-750	20	386	#	73	155	#	10	S10
Co/CeO_2 Co/TiO2 Co/ZrO2	150 120 100	365 390 373	#	65.0 67.9 70.8	11.15 7.93 5.63	0.0063 @361 @353 @349	3	S11
CoP/NiCoP	140	310	1.63	104.5	#	#	24	S12
CoOOH-CS/NF	**1595**	**311**	**1.90** @100	**96.9**	**33.5**	**0.005**	**100**	**This work**
NiFe based catalysts								
NiFe-LDH/CNT	40	300	1.477	31	#	0.56	1	S13
$Fe_{0.1}Ni_{0.9}O$	40	297	#	37	0.35	1.9	10	S14
$Ni_{0.9}Fe_{0.1}$/NC	80	330	1.58	45	#	#	24	S15
$Fe_{0.5}Ni_{0.5}O_x$	25	584	#	72	#	#	1.5	S16
$Ni_3Fe(OH)_9/Ni_3Fe$	150	280	1.63	28	#	0.083	24	S17
Ni-Fe-NP	500	210	1.55	53	31	0.052	24	S18
a-LNFBPO@NF	450	215	#	37	39.6	0.572	300	S19
$Ni_{1-x}Fe_x(OH)_y$-CS/NF	**1750**	**275**	**1.89** @100	**71**	**34.7**	**0.007**	**100**	**This work**

[#]Not reported.

References

S1. G. Dong, M. Fang, J. Zhang, R. Wei, L. Shu, X. Liang, S. Yip, F. Wang, L. Guan, Z. Zheng and J. C. Ho, *J. Mater. Chem. A*, 2017, **5**, 11009–11015.

S2. T. Dhanasekaran, A. Bovas and T. P. Radhakrishnan, *ACS Appl. Mater. Interfaces*, 2023, **15**, 6687–6696.

S3. C. Meng, M. Lin, X. Sun, X. Chen, X. Chen, X. Du and Y. Zhou, *Chem. Commun.*, 2019, **55**, 2904–2907.

S4. Q. S. Jiang, W. Li, J. Wu, W. Cheng, J. Zhu, Z. Yan, X. Wang and Y. Ju, *J. Mater. Sci. Mater. Electron.*, 2019, **30**, 9429–9437.

S5. C. Liu, H. Zhu, Z. Zhang, J. Hao, Y. Wu, J. Guan, S. Lu, F. Duan, M. Zhang and M. Du, *Sustain. Energy Fuels*, 2019, **3**, 3518–3524.

S6. C. C. L. McCrory, S. Jung, J. C. Peters and T. F. Jaramillo, *J. Am. Chem. Soc.*, 2013, **135**, 16977–16987.

S7. J. Huang, J. Chen, T. Yao, J. He, S. Jiang, Z. Sun, Q. Liu, W. Cheng, F. Hu, Y. Jiang, Z. Pan and S. Wei, *Angew. Chem.*, 2015, **127**, 8846–8851.

S8. X. Li, Z. Niu, J. Jiang and L. Ai, *J. Mater. Chem. A*, 2016, **4**, 3204–3209.

S9. L. K. Wu, W. Y. Wu, J. Xia, H. Z. Cao, G. Y. Hou, Y. P. Tang and G. Q. Zheng, *J. Mater. Chem. A*, 2017, **5**, 10669–10677.

S10. Q. Zhang, Z. Duan, M. Li and J. Guan, *Chem. Commun.*, 2020, **56**, 794–797.

S11. M. Akbayrak and A. M. Önal, *Electrochim. Acta*, 2021, **393**, 139053.

S12. X. Fu, Z. Zhang, Y. Zheng, J. Lu, S. Cheng, J. Su, H. Wei and Y. Gao, *J. Colloid Interface Sci.*, 2024, **653**, 1272–1282.

S13. M. Gong, Y. Li, H. Wang, Y. Liang, J. Z. Wu, J. Zhou, J. Wang, T. Regier, F. Wei and H. Dai, *J. Am. Chem. Soc.*, 2013, **135**, 8452–8455.

S14. K. Fominykh, P. Chernev, I. Zaharieva, J. Sicklinger, G. Stefanic, M. Doblinger, A. Muller, A. Pokharel, S. Bocklein, C. Scheu, T. Bein and D. Fattakhova-Rohlfing, *ACS Nano*, 2015, **9**, 5180–5188.

S15. X. Zhang, H. Xu, X. Li, Y. Li, T. Yang and Y. Liang, *ACS Catal.*, 2016, **6**, 580–588.

S16. J. Jiang, C. Zhang and L. Ai, *Electrochim. Acta*, 2016, **208**, 17–24.

S17. C. Xiao, X. Zhang, S. Li, B. H. R. Suryanto and D. R. MacFarlane, *ACS Appl. Energy Mater.*, 2018, **1**, 986–992.

S18. B. H. R. Suryanto, Y. Wang, R. K. Hocking, W. Adamson and C. Zhao, *Nat. Commun.*, 2019, **10**, 5599.

S19. J. Kwon, H. Han, S. Jo, S. Choi, K. Y. Chung, G. Ali, K. Park, U. Paik and T. Song, *Adv. Energy Mater.*, 2021, **11**, 2100624.